Frequency shift in an oscillator with photorefractive gain

L. Dambly and H. Zeghlache
Laboratoire de Spectroscopie Hertzienne, Université des Sciences et Technologies de Lille1, 59655 Villeneuve d'Ascq CEDEX, France
(Received 24 June 1992)

A self-consistent theory is used to derive the frequency shift presented by the oscillating mode in a cavity that contains a photorefractive crystal. A long-time-limit theory has been used to get the steady characteristics of the cavity field. The problem of the weak-field approximation is avoided. This approximation is useless in the case studied because the interaction along the crystal is so strong that one has to take in account the intensity exchange occurring inside the material between the pump and oscillating beams (two-wave mixing). We have fully analyzed the influence of the transverse nature of the beams on the intensity exchange in the two-wave mixing situation. In the photorefractive resonator case, the frequency shift of the oscillating beam is expressed in terms of a ratio that presents poles. The dependence on the problem parameters of these poles is studied and a perturbative method is developed; it is based on the smallness of the transverse overlap between the pump and cavity modes. An analytical expression for this frequency shift is obtained.

PACS number(s): 42.65.Hw

I. INTRODUCTION

Photorefractive (PR) materials were first used in optical signal processing, dynamic holography, storage media in holographic memory systems [1–4], phase conjugation [5–8], and more recently in photorefractively pumped oscillators in a ring cavity or a Fabry-Pérot étalon [9]. This kind of oscillator is based on the photorefractive gain (as an interaction between light and matter) and on oscillation in a cavity. It has spurred new devices and phenomena and some review papers concerning these two topics have been published: the photorefractive oscillator is largely studied by Kwong, Cronin-Golomb, and Yariv [10] and the two-wave mixing in a photorefractive material is developed by Yeh [11] and in [12–14]. This paper is devoted to the theory describing such an oscillator.

Photorefractive materials are well known for the important mode-pulling frequency they induce during the two-wave mixing operation. The frequency shift of the active mode with respect to the pump frequency has been experimentally measured and found to be a few hertz [15,16]. Since the crystal gain line, centered around the pump frequency, has a linewidth of a few hertz for $BaTiO_3$, for example [a few hundreds of hertz for BGO (bismuth silicon oxide)], the measured values express the oscillation condition imposed on the mode and can represent a frequency shift that the probe beam undergoes. In a ring cavity configuration where passive modes of the empty cavity exist, the photorefractive oscillator presents a dynamical behavior that clearly signs the presence of this pulling effect: it shows a nearly continuous succession of the transverse cavity modes defining a periodic alternation and also a turbulent behavior when the modes number in the cavity increases (see, for example, Refs. [16,17]). This spatiotemporal behavior occurring on a time scale related to the material characteristic time (1 ms) rather than the cavity time (10^{-8} s), and based on this dynamically strong frequency pulling, is due to the photorefractive nonlinearity connecting the oscillating field and the matter. In this theoretical paper we want to demonstrate that such an important pulling can be realized for a suitable parametric situation. We choose to model the simplest configuration [18]: several oscillators using various photorefractive materials have been tried [9,19, and references quoted therein]. From the theoretical point of view, the method used to describe the PR oscillator is similar to the Lamb self-consistent theory derived for the lasers. The field present in the cavity is partially (with the pump beam) responsible for the material index grating. The nonlinear polarization induced in the medium acts as a source term for the resonator field in accordance with the Maxwell equations. This method has been used recently by Anderson and Saxena [19] and D'Alessandro [20] to describe the dynamics of the photorefractive oscillator. The first paper [19] presents a theory for a multimode oscillation using the weak-field limit; the pump depletion and the intermode gratings are neglected. The modulation index of the intensity pattern is also supposed to remain small. This model is very similar to the laser description and it produces the same results, for example, a mode-competition phenomenon which is stronger for modes having similar transverse distribution. The second paper [20] presents a study of the dynamics in the transverse plane. The author also uses the weak-field limit and obtains a laserlike description, but since the material variable is very slow, the model can be reduced. A spatiotemporal numerical analysis is then performed using the Gauss-Laguerre modes expansion: the set of partial differential equations is boiled down to a set of ordinary differential equations and 55 Gauss-Laguerre modes, at least, are involved in the description. The results are very similar to those of the transverse laser patterns, except that the time scale corresponds to the material characteristic time. Our goal

is slightly different from the previous works: we are not yet concerned with the dynamics of the photorefractive oscillator even if it is our final aim. However, since the weak-field limit is invalid for most experimental situations, one needs to integrate into the description the longitudinal (or the oscillating field propagation direction) intensity exchanges that occur inside the crystal, the transverse nature of the fields, and finally to define more closely the nonlinearities. Because of the difficulty and the length of such a study, we only present in this paper a qualitative and steady analysis leading to the frequency of the oscillating field. This paper is organized as follows. In Sec. II, we develop a cavity model following the first work of Yariv and Kwong [21]. We use the Maxwell equations to describe the cavity oscillating field and proceed to an expansion in terms of the empty cavity transverse modes. The nonlinear polarization, acting as a source term for the field, is produced inside the crystal by the coupling between the oscillating field and a pump beam via the electro-optic effect. Section III will be devoted to express this photorefractive coupling using the rate equations of the Kukhtarev approach [22]. The power exchange between the pump and the oscillating field along the crystal length is considered including the longitudinal dependence of the fields. One then needs to solve the two-beam coupling problem in the PR crystal for one passage and the influence of transverse field characteristics on the intensity exchange. This is developed in Sec. IV. All the elements needed to solve the steady problem are presented. Returning to cavity model, we deduce in Sec. V the frequency shift the oscillating field undergoes which is due to the optical activity of the photorefractive material. Numerical simulations will give a description of the frequency pulling versus the problem parameters.

II. CAVITY MODEL

The system we model is represented in the scheme of Fig. 1. Two coherent beams $\mathbf{E}_p(\mathbf{r},t)$ and $\mathbf{E}(\mathbf{r},t)$ interfere inside a photorefractive crystal: $\mathbf{E}_p$ is the pump beam and $\mathbf{E}$ is the probe and also the oscillating field. The two beam directions are symmetric with respect to the normal to the crystal input surface and are separated by 2θ. To obtain sustained oscillations of the field $\mathbf{E}$, the system is placed in a ring cavity. We give a general treatment of this self-consistent method and following the approach presented by Kwong, Cronin-Golomb, and Yariv in Ref. [10] we expand the oscillating field on the complete set of the transverse empty resonator electric and magnetic modes $\mathbf{E}_a$ and $\mathbf{H}_a$:

$$\mathbf{E}_p(\mathbf{r},t)=\mathbf{E}_p(\mathbf{r}_\perp,z,t)=-\frac{1}{\sqrt{\epsilon}}p_0(z,t)\mathbf{E}_0(\mathbf{r}) ,$$

$$\mathbf{E}(\mathbf{r},t)=-\frac{1}{\sqrt{\epsilon}}\sum_{a=1}^{\infty}p_a(z,t)\mathbf{E}_a(\mathbf{r}) , \quad (1)$$

$$\mathbf{H}(\mathbf{r},t)=\frac{1}{\sqrt{\mu}}\sum_{a=1}^{\infty}\omega_a q_a(z,t)\mathbf{H}_a(\mathbf{r}) ,$$

where $\mathbf{r}=(r_\perp,z)$. The p's and q's are the expansion coefficients on the basis set. They contain the characteristics introduced by the crystal presence, which we reduce to the longitudinal dependence. The $\mathbf{E}_a$'s and $\mathbf{H}_a$'s represent the free propagation in the empty cavity.

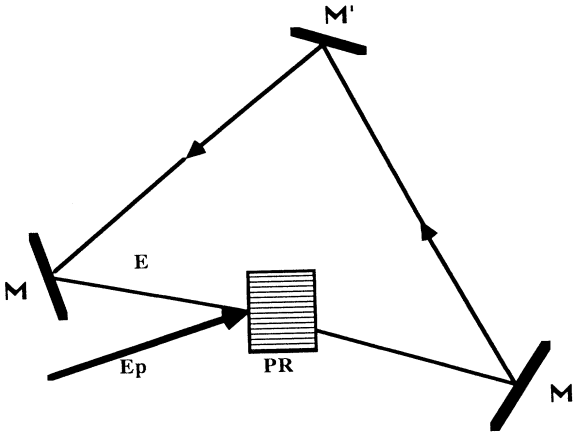

FIG. 1. Simplified scheme of the self-induced optical ring cavity with a photorefractive amplifier.

Experimentally the crystal must be uniformly illuminated: the transverse characteristics of the pump beam are those of the plane wave. The electric and magnetic permittivities are ϵ and μ ($\approx\mu_0$). The a index holds the characteristics of the eigenstates of the empty cavity. The frequencies ω_a are the related passive eigenfrequencies. Following the boundary conditions, the eigenstates can be expressed differently. As an example, the resonator transverse modes $\mathbf{E}_a$ are proportional to the Gauss-Laguerre polynomials when the transverse Laplacian is taken in cylindrical coordinates, and one can use the following notations: $a=N$ (for the longitudinal coordinate z), p, l, and i (for the transverse coordinates) [20,23]. They can have also another mathematical expression depending on the dominant symmetry of the considered system: for a cartesian symmetry, one can use the Gauss-Hermite polynomials. These transverse modes verify several properties, such as the orthonormality of a complete set

$$\int_{V_{\text{cav}}}\mathbf{E}_a^*(\mathbf{r})\cdot\mathbf{E}_b(\mathbf{r})dV=\delta_{ab} ,$$

$$\int_{V_{\text{cav}}}\mathbf{H}_a^*(\mathbf{r})\cdot\mathbf{H}_b(\mathbf{r})dV=\delta_{ab} ,$$

where V_{cav} stands for an integration over all the cavity volume and

$$\nabla\times\mathbf{E}_a=k_a\mathbf{H}_a, \quad \nabla\times\mathbf{H}_a=k_a\mathbf{E}_a , \quad (2)$$

where $k_a=\omega_a\sqrt{\epsilon\mu}$.

The main difference with previous papers [21] is the explicit z dependence of the p and q coefficients, meaning that we keep the power exchange between the pump and the probe beams which mainly occurs in the crystal. These exchanges are important enough to make invalid, in some sense, the mean-field limit (or weak-field limit) as it is used in the laser case: for example, if the losses are neglected, a total energy transfer can occur between the two beams during one passage along a photorefractive

medium of a centimeter length. This energy transfer is held in the nonlinear contribution as follows.

The nonlinear influence of the crystal can be included in a polarization $\mathbf{P}$ following the expression $\mathbf{P}=\epsilon_0\chi\mathbf{E}+\mathbf{P}_{\rm NL}$, where χ is the medium linear electric susceptibility. The Maxwell equations applied to the electromagnetic field in the cavity can be written as

$$\nabla\times\mathbf{H}=\sigma\mathbf{E}+\epsilon\frac{\partial\mathbf{E}}{\partial t}+\frac{\partial\mathbf{P}_{\rm NL}}{\partial t}\ ,$$
$$\nabla\times\mathbf{E}=-\mu_0\frac{\partial\mathbf{H}}{\partial t}\ . \tag{3a}$$

The resonator fields equations are taken as source-free equations which can be justified by the fact that, although there may be charges in the photorefractive material, the charges are not free at times comparable with an optical period. We have used the constitutive relations linking the fields $\mathbf{E}$ and $\mathbf{B}$ to the material quantities $\mathbf{D}$, $\mathbf{H}$, and $\mathbf{J}$ following

$$\mathbf{D}=\epsilon_0\mathbf{E}+\mathbf{P},\quad \mathbf{B}=\mu_0\mathbf{H},\quad \mathbf{J}=\sigma\mathbf{E}\ . \tag{3b}$$

Introducing the modal expansion (1), we get

$$\sum_{a=1}^{\infty}\left\{\frac{\omega_a}{\sqrt{\mu}}[k_a q_a\mathbf{E}_a+\mathbf{H}_a\times\nabla q_a]+\frac{\sigma}{\sqrt{\epsilon}}p_a\mathbf{E}_a+\sqrt{\epsilon}\mathbf{E}_a\frac{\partial p_a}{\partial t}\right\}=\frac{\partial\mathbf{P}_{\rm NL}}{\partial t}\ , \tag{4a}$$

$$\sum_{a=1}^{\infty}\left\{\mathbf{E}_a\times\nabla p_a+k_a\mathbf{H}_a\left[p_a-\frac{\partial q_a}{\partial t}\right]\right\}=0\ . \tag{4b}$$

Outside the crystal, no longitudinal transfer occurs and one can neglect ∇p_a and ∇q_a. Equation (4b) leads to the relation $p_a=\partial_t q_a$ for each index a. Inside the crystal, this condition is still valid as a first order of an approximation that leads to neglect the transverse contributions: if one compares the contribution of each component of Eqs. (4b) and (4a) for experimental situations, the ∇ terms due to the crystal nonlinearity are negligible with respect to the k_a terms. To get a self-consistent field equation, a time derivation is performed on Eq. (4a) that gives

$$\sum_{a=1}^{\infty}\left\{\frac{\omega_a}{\sqrt{\mu}}k_a p_a\mathbf{E}_a+\frac{\sigma}{\sqrt{\epsilon}}\mathbf{E}_a\frac{\partial p_a}{\partial t}+\sqrt{\epsilon}\mathbf{E}_a\frac{\partial^2 p_a}{\partial t^2}\right\}\cong\frac{\partial^2\mathbf{P}_{\rm NL}}{\partial t^2}\ . \tag{5}$$

We can then make a projection on one mode of the cavity, say $\mathbf{E}_d$, by multiplying Eq. (5) by $\mathbf{E}_d^*$ and integrating over the volume of the cavity. Using the orthonormality relation verified by the cavity modes and neglecting the partial integration over the crystal with respect to the integration outside the crystal, we get the following equation for each mode:

$$\omega_d^2 p_d+\frac{\sigma}{\epsilon}\frac{\partial p_d}{\partial t}+\frac{\partial^2 p_d}{\partial t^2}\cong\frac{1}{\sqrt{\epsilon}}\frac{\partial^2}{\partial t^2}\int_{V_{\rm crys}}\mathbf{E}_d^*(\mathbf{r})\cdot\mathbf{P}_{\rm NL}(z,t)dV \tag{6a}$$

or

$$\omega_d^2 p_d+\frac{\omega_d}{Q_d}\frac{\partial p_d}{\partial t}+\frac{\partial^2 p_d}{\partial t^2}\cong\frac{1}{\sqrt{\epsilon}}\frac{\partial^2}{\partial t^2}\int_{V_{\rm crys}}\mathbf{E}_d^*(\mathbf{r})\cdot\mathbf{P}_{\rm NL}(z,t)dV\ , \tag{6b}$$

where the resonator quality factor for the d mode is defined as $Q_d=\omega_d(\epsilon/\sigma)$. On the right-hand side of Eqs. (6), we have reduced the integration volume to the crystal volume because all the nonlinearities are limited to the crystal dimensions. The equation that we get is similar to that of Ref. [21] except for the z dependence of the p_d's contained in $\mathbf{P}_{\rm NL}(z,t)$.

The field source $\mathbf{P}_{\rm NL}$ in Eq. (6) represents any interaction between the field and matter, thus this equation is general. We presently have to specify the photorefractive nature of the nonlinearity.

III. PHOTOREFRACTIVE COUPLING

The nonlinear polarization $\mathbf{P}_{\rm NL}$ driving the oscillation of the resonator field is that produced by the incidence of the input field $\mathbf{E}_p(\mathbf{r},t)$ on the index grating created photorefractively by the interaction between $\mathbf{E}_p(\mathbf{r},t)$ and $\mathbf{E}(\mathbf{r},t)$. The charges in the nonuniformly illuminated photorefractive medium migrate in the presence of light, creating a space-charge field and hence an index change via the electro-optic coefficient of the material. The nonlinear polarization takes the form

$$\mathbf{P}_{\rm NL}(\mathbf{r},t)=\epsilon_0\Delta n(\mathbf{r},t)\mathbf{E}_p(\mathbf{r},t)\ , \tag{7}$$

where ϵ_0 is the vacuum dielectric constant, $\Delta n(\mathbf{r},t)$ is the index grating formed by the input beam and oscillating field interference. In the Kukhtarev formulation [19,22], based on steady rate equations, the index grating can be written as

$$\Delta n(\mathbf{r},t)=\frac{2c}{\epsilon}\sum_{a=1}^{\infty}\frac{\gamma}{\omega_a'}\frac{p_0^*(z,t)p_a(z,t)[\mathbf{E}_0^*(\mathbf{r})\cdot\mathbf{E}_a(\mathbf{r})]}{I_T(\mathbf{r},t)}\ , \tag{8}$$

where the numerator expresses the vectorial coupling (interference) of the pump with each of the modes of the probe beam (the brackets stand for a scalar product). This expression is derived for two-wave mixing in a crystal placed in a suitable position along the wave propagation direction. The denominator follows the notations of Refs. [10,19,21] and is given by

$$I_T(\mathbf{r},t)=\frac{1}{\epsilon}|p_0(z,t)\mathbf{E}_0(\mathbf{r})|^2+\frac{1}{\epsilon}\sum_{a=1}^{\infty}|p_a(z,t)\mathbf{E}_a(\mathbf{r})|^2\ . \tag{9}$$

It represents a kind of normalization of the refractive index. This has no physical justification to our knowledge. For two-plane wave mixing realized in such materials, the usually dimensionless refractive index is normalized with the total intensity: without absorption this is the conserved quantity of the problem. However, in a more general description involving the transverse dimensions of the modes, the refractive index normalization is still an opened problem from the nonlinear point of view. In our

case, we have kept the total intensity and remark that it can be taken outside the summation in Eq. (8). We also note that the active model frequency is ω'. From the stationary standard photorefractive theory involving two beams $E_p(\omega_p)$ and $E(\omega')$, the Pockels effect is at the origin of the coupling. By identifying the microscopic details of the photorefractive process and the three different mechanisms that can affect the motion of the photoexcited carriers, the complex coupling constant γ takes the form [10,21]

$$\gamma=\frac{\omega' r_{\text{eff}} n_0^3}{4c}\frac{E_q(E_{\text{ext}}+iE_D)}{[E_{\text{ext}}-t_0(E_D+E_\mu)(\omega'-\omega_p)]+i[E_D+E_q+t_0E_{\text{ext}}(\omega'-\omega_p)]}\ , \tag{10}$$

where the following notations have been used: r_{eff} is the relevant electro-optic coefficient, n_0 the ordinary refractive index of the crystal, $t_0=N_A/(\alpha_D N I_0)$ the characteristic time in the crystal, N_A the concentration of the trapping centers, α_D the intensity cross-section coefficient, E_{ext} the externally applied dc electric field, and E_μ, E_D, and E_q the internal electric fields due to drift, diffusion, and maximum space-charge, respectively. These parameters can be deduced from the crystal properties and orientation with respect to the interacting beams. The coupling constant being a complex expression, it can be taken in polar representation as $\Gamma e^{+i\Phi}$, where Φ is the phase mismatch between the wave interference grating and the refractive index grating. One can control this parameter via the externally applied electric field E_0. In the Yariv-Kwong description [21], this parameter is around $\pi/2$ because they use a $BaTiO_3$ crystal: the main microscopic process occurring in the system is the diffusion. In that case, the intensity transfer between the beams is maximum, but the phase spatial evolution is frozen [see Sec. IV, Eqs. (37) and (38)]. Returning to our problem and including Eqs. (7) and (8) in Eq. (6), we obtain

$$\omega_d^2 p_d+\frac{\omega_d}{Q_d}\frac{\partial p_d}{\partial t}+\frac{\partial^2 p_d}{\partial t^2}\cong-\frac{2c\epsilon_0}{\epsilon^2}\sum_{a=1}^{\infty}\frac{\gamma}{\omega_a'}\frac{\partial^2}{\partial t^2}\int_{V_{\text{crys}}}|p_0(z,t)|^2 p_a(z,t)\times\frac{[\mathbf{E}_d^*\cdot\mathbf{E}_0][\mathbf{E}_0^*\cdot\mathbf{E}_a]}{I_T(\mathbf{r},t)}dV\ . \tag{11}$$

The integral occurs over the z and transverse components. The following step concerns the time dependence of the p components: one can subtract the optical oscillation term through the relations

$$p_0(z,t)=\not{p}_0(z,t)e^{i\omega_p t},\quad p_a(z,t)=\not{p}_a(z,t)e^{i\omega_a' t}$$

and release the slowly varying unknown amplitude in the $\not{p}_a$ terms. In this situation, the ω_a' are the active mode frequency (to be distinguished from ω_a, which are the passive cavity frequencies). Then Eq. (11) can be written as

$$\left[(\omega_d^2-\omega_d'^2)+i\frac{\omega_d\omega_d'}{Q_d}\right]\not{p}_d+\left[\frac{\omega_d}{Q_d}+2i\omega_d'\right]\frac{\partial\not{p}_d}{\partial t}+\frac{\partial^2\not{p}_d}{\partial t^2}\cong-\frac{2c\epsilon_0}{\epsilon^2}e^{-i\omega_d' t}\sum_{a=1}^{\infty}\frac{\gamma}{\omega_a'}\frac{\partial^2}{\partial t^2}e^{i\omega_a' t}\int_{V_{\text{crys}}}|\not{p}_0(z,t)|^2\not{p}_a(z,t)\frac{[\mathbf{E}_d^*\cdot\mathbf{E}_0][\mathbf{E}_0^*\cdot\mathbf{E}_a]}{I_T(\mathbf{r},t)}dV\ , \tag{12}$$

where $I_T(\mathbf{r},t)$ has the same form as in Eq. (9) and the p variables are replaced.

Our task in this paper is to get the frequency of the oscillating beam. For the multimode oscillation, this stationary model can be used, but only for degenerate modes. Otherwise the beating terms between the d mode and the other transverse components of the oscillating field exclude any complete stationary theory.

At this stage, we consider a monomode situation. The oscillating transverse mode is the d mode. Then Eq. (12) takes an easier form. In the long-time limit the steady state is reached: $\not{p}_0(z,t)=\not{p}_0(z)$ and $\not{p}_d(z,t)=\not{p}_d(z)$. The time derivatives of $\not{p}$ vanish and we get at first order

$$\left[(\omega_d^2-\omega_d'^2)+i\frac{\omega_d\omega_d'}{Q_d}\right]\not{p}_d\cong\frac{2c\epsilon_0}{\epsilon}\gamma\omega_d' F\ , \tag{13}$$

where

$$F=\int_0^L dz\,|\not{p}_0(z)|^2\not{p}_d(z)\times\int d\mathbf{r}_\perp\frac{|\mathbf{E}_d^*\cdot\mathbf{E}_0|^2}{|\not{p}_0(z)\mathbf{E}_0|^2+|\not{p}_d(z)\mathbf{E}_d|^2} \tag{14}$$

and L is the crystal length. We note that Eq. (14) gives a constant value with respect to space, while in Eq. (13), the $\not{p}_d$ variable is taken outside the crystal such that one can consider its value at either $z=0$ or L. To perform the z integration we need to know $\not{p}(z)$. We choose to derive this dependence using a single-passage model through the crystal. This can be justified in the long-time limit compared to the crystal characteristic time. In the next section we shall focus on the single passage through the photorefractive medium.

IV. TWO-BEAM COUPLING THEORY

In this section we describe the passage through the PR crystal of the two beams $\mathbf{E}_p(\mathbf{r},t)$ and $\mathbf{E}(\mathbf{r},t)$. We start with the wave equation for each field. The input and probe fields are governed by the following wave equations:

$$\begin{aligned}\Delta\mathbf{E}(\mathbf{r},t)-\sigma\mu_0\frac{\partial\mathbf{E}}{\partial t}-\mu_0\epsilon\frac{\partial^2\mathbf{E}}{\partial t^2}&=\mu_0\frac{\partial^2\mathbf{P}_{\mathrm{NL}}}{\partial t^2}\ ,\\ \Delta\mathbf{E}_p(\mathbf{r},t)-\sigma\mu_0\frac{\partial\mathbf{E}_p}{\partial t}-\mu_0\epsilon\frac{\partial^2\mathbf{E}_p}{\partial t^2}&=\mu_0\frac{\partial^2\mathbf{P}'_{\mathrm{NL}}}{\partial t^2}\ ,\end{aligned} \tag{15}$$

and use the transverse expansions of Eq. (1). The expressions

$$\begin{aligned}\mathbf{E}_a(\mathbf{r})&=\mathbf{E}_{a\perp}(\mathbf{r}_\perp)e^{i(\omega'_a t-k_a z)}\ ,\\ \mathbf{E}_0(\mathbf{r})&=\mathbf{E}_{0\perp}(\mathbf{r}_\perp)e^{i(\omega_p t-k_p z)}\end{aligned} \tag{16}$$

directly subtract the optical frequencies, keep the slowly varying amplitudes $\mathcal{A}$, and separate the z and the $r_\perp$ dependences: the smallness of the crystal length with respect to the Rayleigh length allows us to neglect the z dependence of the $\mathbf{E}_a(\mathbf{r}_\perp)$'s [21,23]. Using the slowly varying amplitude approximation $[(\partial^2\mathcal{A}/\partial z^2)\ll k(\partial\mathcal{A}/\partial z)]$, the transverse eigenvector definition, and keeping in mind the stationary case $[\mathcal{A}(z,t)=\mathcal{A}(a)]$, one easily gets for the two beams

$$\sum_{a=1}^{\infty}\mathbf{E}_{a\perp}e^{i(\omega'_a t-k_a z)}\left\{2ik_a\frac{\partial\mathcal{A}_a}{\partial z}+i\omega'_a\sigma\mu_0\mathcal{A}_a+\left[\frac{\partial\mathcal{A}_a}{\partial t}\ \text{terms}\right]\right\}=-\mu_0\sqrt{\epsilon}\frac{\partial^2\mathbf{P}_{\mathrm{NL}}}{\partial t^2}\ , \tag{17a}$$

$$\mathbf{E}_{0\perp}\left\{2ik_p\frac{\partial\mathcal{A}_0}{\partial z}+i\omega_p\mu_0\mathcal{A}_0+\left[\frac{\partial\mathcal{A}_0}{\partial t}\ \text{terms}\right]\right\}e^{i(\omega_p t-k_p z)}=-\mu_0\sqrt{\epsilon}\frac{\partial^2\mathbf{P}'_{\mathrm{NL}}}{\partial t^2}\ . \tag{17b}$$

As in the preceding section, a projection on a transverse mode $\mathbf{E}_{d\perp}$ is performed, leading to

$$2ik_d\frac{\partial\mathcal{A}_d}{\partial z}+i\omega'_d\sigma\mu_0\mathcal{A}_d+\left[\frac{\partial\mathcal{A}_d}{\partial t}\ \text{terms}\right]=-\mu_0 e^{-i(\omega'_d t-k_d z)}\frac{\partial^2}{\partial t^2}\int d\mathbf{r}_\perp[\mathbf{E}^*_{d\perp}\cdot\mathbf{P}_{\mathrm{NL}}]\ , \tag{18a}$$

$$2ik_p\frac{\partial\mathcal{A}_0}{\partial z}+i\omega_p\sigma\mu_0\mathcal{A}_0+\left[\frac{\partial\mathcal{A}_0}{\partial t}\ \text{terms}\right]=-\mu_0\sqrt{\epsilon}e^{-i(\omega_p t-k_p z)}\frac{\partial^2}{\partial t^2}\int d\mathbf{r}_\perp[\mathbf{E}^*_{0\perp}\cdot\mathbf{P}'_{\mathrm{NL}}]\ . \tag{18b}$$

Now the integrals are performed along the crystal transverse dimensions. As before the polarization terms must be expressed. In general, the nonlinear coupling that affects the probe field $\mathbf{E}$ is due to the medium polarization created by the pump field. The polarization term $\mathbf{P}_{\mathrm{NL}}(\mathbf{r},t)$ can be written as

$$\mathbf{P}_{\mathrm{NL}}(\mathbf{r},t)=\epsilon_0\Delta n(\mathbf{r},t)\mathbf{E}_p(\mathbf{r},t)\ . \tag{19a}$$

For the pump field, the medium polarization is due to the probe field

$$\mathbf{P}'_{\mathrm{NL}}(\mathbf{r},t)=\epsilon_0\Delta n^*(\mathbf{r},t)\mathbf{E}(\mathbf{r},t)\ . \tag{19b}$$

In these relations, Δn is given by Eq. (8), completed by Eqs. (9) and (16),

$$\Delta n(\mathbf{r},t)=\frac{2c}{\epsilon}\sum_{a=1}^{\infty}\frac{\gamma}{\omega'_a}e^{i(k_p-k_a)z}e^{i(\omega'_a-\omega_p)t}\times\frac{\mathcal{A}^*_0(z,t)\mathcal{A}_a(z,t)[\mathbf{E}^*_{0\perp}\cdot\mathbf{E}_{a\perp}]}{I_T(\mathbf{r},t)}\ , \tag{20}$$

where the total intensity density is still given by

$$I_T(\mathbf{r},t)=\frac{1}{\epsilon}|\mathcal{A}_0(z,t)\mathbf{E}_{0\perp}|^2+\frac{1}{\epsilon}\sum_{a=1}^{\infty}|\mathcal{A}_a(z,t)\mathbf{E}_{a\perp}|^2\ . \tag{21}$$

We restrict the analysis to a monomode description and in the long-time limit, we get

$$2ik_d\frac{d\mathcal{A}_d}{dz}+i\omega'_d\sigma\mu_0\mathcal{A}_d=2c\mu_0\epsilon_0\gamma\omega'_d|\mathcal{A}_0(z)|^2\mathcal{A}_d(z)G(z)\ , \tag{22a}$$

$$2ik_p\frac{d\mathcal{A}_0}{dz}+i\omega_p\sigma\mu_0\mathcal{A}_0=2c\mu_0\epsilon_0\gamma^*\omega_p|\mathcal{A}_d(z)|^2\mathcal{A}_0(z)G(z)\ . \tag{22b}$$

The function G is directly related to the transverse characteristics of the beam and also contains the refractive index normalization. It is given by

$$G(z)=\int d\mathbf{r}_\perp\frac{|\mathbf{E}^*_{d\perp}\cdot\mathbf{E}_{0\perp}|^2}{|\mathcal{A}_0(z)\mathbf{E}_{0\perp}|^2+|\mathcal{A}_d(z)\mathbf{E}_{d\perp}|^2}\ . \tag{23}$$

One can note the evident relation between Eqs. (14) and (23). The crystal smallness compared to the Rayleigh length has been used here to get rid of the complexity since the z dependence in the denominator is well located in G: the spatial dependences are separated and one can write

$$|\mathcal{A}(z)\mathbf{E}_\perp|^2=|\mathcal{A}(z)|^2|\mathbf{E}_\perp|^2\ . \tag{24}$$

We note that k_p and k_d are the z components of the wave vectors inside the medium. They are given by the following expressions:

$$k_p=\frac{2\pi}{\lambda_p}n_0\cos(\theta),\quad k_d=\frac{2\pi}{\lambda_d}n_0\cos(\theta)\ . \tag{25}$$

For convenient notation, we take $\lambda_p=\lambda_d=\lambda$, which corresponds to fixed fringe patterns. But even if $\lambda_p\neq\lambda_d$, the medium response time is so slow that this difference is neglected [11]. We also take $\alpha=c\sigma\mu_0$, the linear absorption coefficient in the PR, and use the following notation:

$$z'=\frac{z}{\cos(\theta)},\quad kn_0=\frac{\omega}{c}=\frac{2\pi}{\lambda}n_0,\quad \gamma=\Gamma e^{+i\phi}, \tag{26}$$

where Γ is the gain factor and ϕ is the phase mismatch between the beams and material gratings. One gets finally

$$\frac{d\mathcal{A}_d}{dz'}+\frac{\alpha}{2}\mathcal{A}_d=-i\frac{\Gamma}{2}e^{+i\phi}|\mathcal{A}_0(z')|^2\mathcal{A}_d(z')G(z'), \tag{27a}$$

$$\frac{d\mathcal{A}_0}{dz'}+\frac{\alpha}{2}\mathcal{A}_0=-i\frac{\Gamma}{2}e^{-i\phi}|\mathcal{A}_d(z')|^2\mathcal{A}_0(z')G(z'), \tag{27b}$$

and can use the polar expansion of the form

$$\mathcal{A}_0=\sqrt{I_0}e^{+i\psi_0},\quad \mathcal{A}_d=\sqrt{I_d}e^{+i\psi_d}.$$

Since G has real values, we finally deal with the following real equations for the intensities and the phases:

$$\frac{dI_0}{dz'}+\alpha I_0=-\Gamma\sin(\phi)I_0I_dG(z'), \tag{28a}$$

$$\frac{dI_d}{dz'}+\alpha I_d=\Gamma\sin(\phi)I_dI_0G(z'), \tag{28b}$$

$$\frac{d\psi_0}{dz'}=\Gamma'\cos(\phi)I_dG(z'), \tag{29a}$$

$$\frac{d\psi_d}{dz'}=\Gamma'\cos(\phi)I_0G(z'). \tag{29b}$$

The parameter Γ is twice Γ'. We note that whatever the function G, the relation $[\partial_{z'}+\alpha](I_d+I_0)=0$ is verified: the total transverse average intensity is conserved for weak losses. For $\phi=\pi/2$, $\psi_{d,0}(z')=\psi_{d,0}(0)$.

At this stage we introduce an approximation that we can justify by the following arguments. As G is related to the normalization factor, its dimension must be an intensity inverse. It also expresses the transverse overlap between the two beams. Thus we propose to approach it by the following expression:

$$G(z')=\frac{1}{|\mathcal{A}_0(z')|^2+f_d|\mathcal{A}_d(z')|^2}. \tag{30}$$

Intuitively we conserve a kind of "total intensity," but the transverse mode intensity is weighted by some coefficient directly related to its transverse profile. In a multimode description, one can easily generalize this idea, since each transverse mode has its own space occupation. We have verified numerically this assumption by integrating the exact Eqs. (27) for several cavity modes characterized by $p=0,1,2,3$ and $l=0,1,2,\ldots,7$. We have calculated the f_d values for which the intensity z profile corresponds to the approximated case profile with an accuracy less than 1%. The results are displayed in Table I and Fig. 2. One can note qualitatively the decreasing values of f_d as p or l increases, more pronounced for $p=0$. This is easily understood if we remind the reader that $\mathbf{E}_{0\perp}$ is a Gaussian function transversally much larger than the cavity mode. As the transverse index increases, this corresponds to multispots patterns: the overlap integral $G(z')$ decreases, and the weight parameter f_d seems to follow.

These low values that we have obtained for the f_d are also related to the transverse nature of the chosen $\mathbf{E}_{0\perp}$. If one considers another $\mathbf{E}_{0\perp}$ profile, the calculated f_d can be quite different and may approach unity: in case of a plane-wave probe field, the f_d value is unity and one finds again the usual equations [11] which give the z evolution of the plane waves inside the crystal. The approximation applied to Eq. (23), which leads to Eq. (30), can also be used in Eq. (14) since the integration occurs only on the crystal: the arguments related to the crystal length are also valid there.

TABLE I. Values of the f_d parameter for different cavity transverse modes.

	$p=0$	$p=1$	$p=2$	$p=3$
$l=0$	0.0776	0.0385	0.0264	0.0204
$l=1$	0.0586	0.0367	0.0274	0.0223
$l=2$	0.0442	0.0295	0.0229	0.0191
$l=3$	0.0369	0.0254	0.0202	0.0170
$l=4$	0.0323	0.0227	0.0182	0.0154
$l=5$	0.0291	0.0207	0.0168	0.0143
$l=6$	0.0267	0.0192	0.0156	0.0134
$l=7$	0.0248	0.0179	0.0147	0.0127

We can solve Eqs. (28) and define a new coupling parameter as $\eta=\Gamma\sin(\phi)$ [$\eta'=\Gamma'\cos(\phi)$] for convenient notation and subtract the loss terms by using the relation

$$I_{0,d}(z')=\bar{I}_{0,d}(z')e^{-\alpha z'}. \tag{31}$$

We get then nearly the same equations as in (28) and using the condition

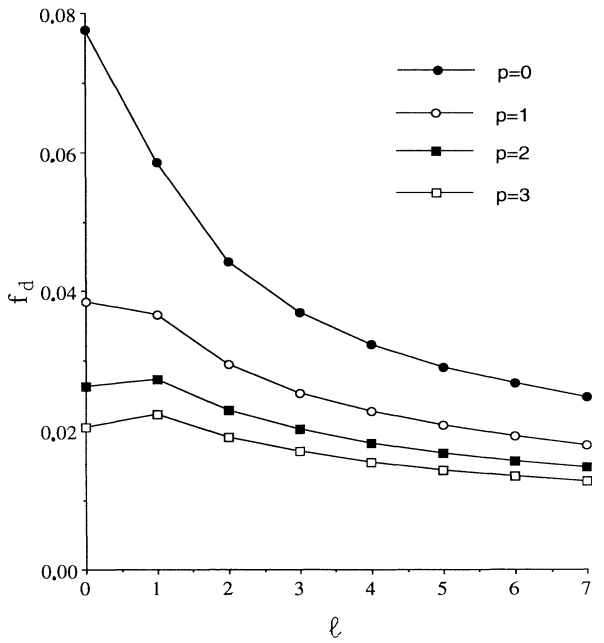

FIG. 2. Validity of the approximation leading to Eq. (30): the f_d values are evaluated when the z profile is obtained using the exact Eq. (25) merged with the profile deduced from the approximated version of Eq. (30).

$$\bar{I}_0(z')+\bar{I}_d(z')=\bar{I}_0(z'=0)+\bar{I}_d(z'=0)=K=\text{const}\ , \quad (32)$$

one can reduce the problem to solving

$$\frac{d\bar{I}_d}{dz'}=\eta\frac{\bar{I}_d(K-\bar{I}_d)}{K+(f_d-1)\bar{I}_d}\ . \quad (33)$$

The exact solution verifies the implicit relation

$$\left[\frac{\bar{I}_d(z')}{\bar{I}_d(0)}\right]\left[\frac{K-\bar{I}_d(0)}{K-\bar{I}_d(z')}\right]^{f_d}=e^{\eta z'}\ . \quad (34)$$

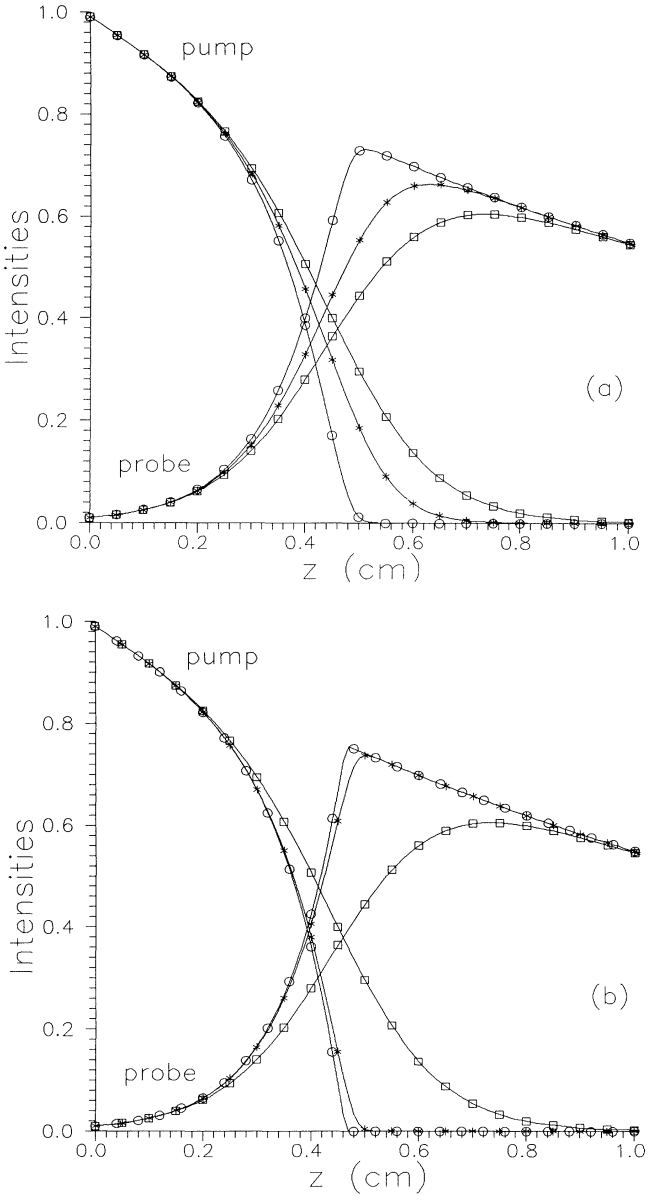

FIG. 3. Solutions of Eq. (28) that give the intensity exchange occurring between the pump and probe beam during one passage in the crystal. The parameters are as follows: (a) $f_d=1$ (squares), 0.5 (asterisks), 0.1 (circles) and (b) $f_d=1$ (squares), 0.0776 (asterisks), 0.0127 (circles). The other parameter values are $\Gamma=10\ \text{cm}^{-1}$ and $\alpha=0.6\ \text{cm}^{-1}$.

We represent in Fig. 3(a) [Fig. 3(b)] the longitudinal evolution of the pump and probe intensities for $f_d=1,0.5$, and 0.1 (1, 0.0776, and 0.0127) and observe that for the same initial condition, the intensity (energy) exchanges occur earlier along the crystal in the non-plane-wave case when compared to the plane-wave case. Figure 3(b) displays the same feature, but for more realistic f_d values: we have taken the extremal values of Table I to get a striking comparison between the different situations. We also observe that all the transverse patterns we have considered give nearly the same intensity exchange. The exchanges are activated: the grating nonlinearity is reinforced by the coupling between two transversely different beams. In the grating interaction, the nonuniform transverse intensity distribution produces a longitudinal increase of the photorefractive gain (due to a variation of the constructive interferences between the beams): mathematically, since f_d takes decreasing values (less than unity), the G contribution becomes larger and the nonlinear term increases. This activates the energy coupling and the exchanges in the crystal.

We can also evaluate from Eq. (33) the maximum value reached by the probe intensity; it is characterized by the following implicit relation:

$$\bar{I}_d(z_c')=\frac{K(1-\alpha)}{1+\alpha(f_d-1)}\ . \quad (35)$$

If we replace Eq. (34) in Eq. (35), we get the position of this maximum along the crystal

$$\eta z_c'=\ln\frac{(1-\alpha)(m^{-1}+1)}{1+\alpha(f_d-1)}-\ln[\alpha(m+1)f_d]\ , \quad (36)$$

where m is defined as $I_d(0)/I_0(0)$. To get the most efficient crystal, the power transfer between the two beams can be optimized by choosing the crystal length.

The knowledge of the intensities is always sufficient to define the phases and solve the phase equations (29). We have found the following relations:

$$\psi_0(z')-\psi_0(0)=-\frac{\eta'}{\eta}\ln\left\{\frac{I_0(z')}{I_0(0)}\right\}-\frac{\eta'}{\eta}\alpha z' \quad (37a)$$

$$=-\frac{\eta'}{\eta}\ln\left\{\frac{K-\bar{I}_d(z')}{K-\bar{I}_d(0)}\right\}\ ,$$

$$\psi_d(z')-\psi_d(0)=\frac{\eta'}{\eta}\ln\left\{\frac{I_d(z')}{I_d(0)}\right\}+\frac{\eta'}{\eta}\alpha z' \quad (37b)$$

$$=\frac{\eta'}{\eta}\ln\left\{\frac{\bar{I}_d(z')}{\bar{I}_d(0)}\right\}\ .$$

We have used the initial relation $\psi_d(0)=(\eta'/\eta)\ln\{\bar{I}_d(0)\}$. For large z', $\bar{I}_d$ increases asymptotically to K and $\bar{I}_0$ to zero. The slope of $\psi_d(d\psi_d/dz')$ becomes zero while the ψ_0 slope is η'/f_d. This is displayed on Fig. 4 for two values of f_d (1 and 0.1). The main difference occurs for ψ_0: at the crystal output, if it is long enough, the transverse nature of the beams has an important influence on the pump beam phase. The wavelength change of the pump beam is more important in case of

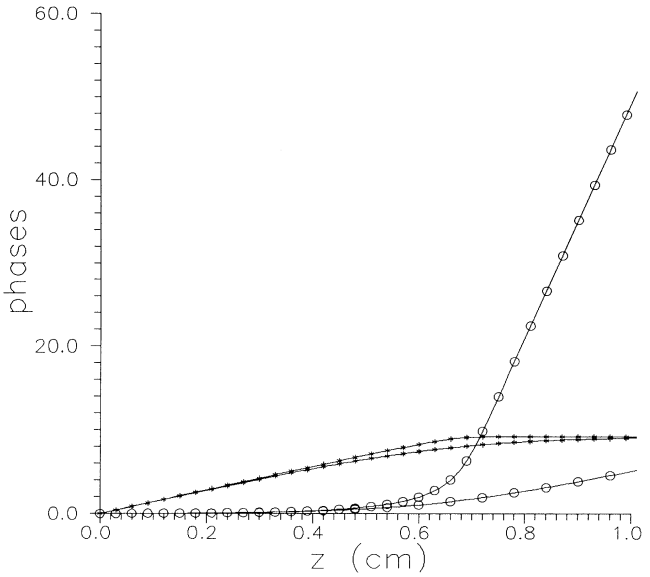

FIG. 4. Solution of Eq. (28) for the phases. The asterisks stand for $\psi_d(z)$, the probe beam phase, while the circles represent $\psi_0(z)$, the pump beam phase. The parameters are $\Gamma=10\ \text{cm}^{-1}$, $\alpha=0.6\ \text{cm}^{-1}$, $\phi=\pi/4$, $I_d(0)=0.01$, and $I_0(0)=0.99$ for all curves, and $f_d=1$ (0.1) for the lower (upper) $\psi_d(z)$ (asterisks) and $\psi_0(z)$ (circles) functions.

transversely complex shapes due to the increase of the nonlinearity (medium refractive index) while the probe beam phase is not affected.

We present in Appendix A two limiting cases of two-wave mixing in a PR crystal that can provide a full analytical study.

These are the general features of the solutions of Eqs. (28) and (29). We have completely characterized the z' dependence of the pump and oscillating fields. At this stage, the numerical way to solve exactly the problem is to go back to Eq. (14), get the F value using the $\mathcal{A}(z')$ derived in this section, insert them in Eq. (13), solve its real and negative parts, and get the frequency shift of the oscillating field. Following this aim, we shall be concerned in the next section with deriving the frequency pulling that the oscillating beam undergoes, using the cavity model of Sec. III.

V. THE FREQUENCY SHIFT OF THE OSCILLATING MODE

We now consider Eqs. (13) and (14). The integral occurs in the crystal only: one can use the approximation (24) followed by (30). We easily obtain

$$\left[(\omega_d^2-\omega_d'^2)+i\frac{\omega_d\omega_d'}{Q_d}\right][I_d(0)e^{+i\psi_d(0)}]^{1/2} = \frac{2c\epsilon 0}{\epsilon}\gamma\omega_d'\int_0^L dz\frac{I_0(z)\sqrt{I_d(z)}e^{+i\psi_d}}{I_0(z)+f_dI_d(z)}\ , \quad (38)$$

where we have taken the oscillating field in $z=0$ for notational simplicity. Using the polar form of γ and the real and imaginary parts of Eq. (38), we obtain the following system:

$$\begin{aligned}(\omega_d^2-\omega_d'^2)\sqrt{I_d(0)} &= \frac{2c\epsilon 0}{\epsilon}\Gamma\omega_d'\int_0^L dz\frac{I_0(z)\sqrt{I_d(z)}}{I_0(z)+f_dI_d(z)} \times\cos\{\psi_d(z)-\psi_d(0)+\phi\}\ ,\\ \frac{\omega_d}{Q_d}\sqrt{I_d(0)} &= \frac{2c\epsilon 0}{\epsilon}\Gamma\int_0^L dz\frac{I_0(z)\sqrt{I_d(z)}}{I_0(z)+f_dI_d(z)} \times\sin\{\psi_d(z)-\psi_d(0)+\phi\}\ .\end{aligned} \quad (39)$$

As in Refs. [10,21] we define t_d the decay time constant of the photon density in the dth mode with no refractive interaction by $1/t_d=\omega_d/Q_d$. This time is much less than the material characteristic time and it is also given by the relation

$$\frac{1}{t_d}=\frac{2c\epsilon 0\Gamma}{\epsilon\sqrt{I_d(0)}}\int_0^L dz\frac{I_0(z)\sqrt{I_d(z)}}{I_0(z)+f_dI_d(z)} \times\sin\{\psi_d(z)-\psi_d(0)+\phi\}\ . \quad (40)$$

We deduce the following expression for the difference:

$$\omega_d^2-\omega_d'^2=\frac{\omega_d'}{t_d}\frac{\mathcal{C}}{\mathcal{S}}\ , \quad (41)$$

where the cosine ($\mathcal{C}$) and sine ($\mathcal{S}$) integrals are given by the expressions

$$\mathcal{C}=\int_0^L dz\frac{I_0(z)\sqrt{I_d(z)}}{I_0(z)+f_dI_d(z)}\cos\{\psi_d(z)-\psi_d(0)+\phi\}\ , \quad (42a)$$

$$\mathcal{S}=\int_0^L dz\frac{I_0(z)\sqrt{I_d(z)}}{I_0(z)+f_dI_d(z)}\sin\{\psi_d(z)-\psi_d(0)+\phi\}\ . \quad (42b)$$

At this stage we remind the reader that the half-linewidth of the material gain line is around a few hertz and the d mode is allowed to oscillate if its active frequency is close to the pump frequency: $\omega_d'\sim\omega_p$. If the frequencies (active and passive) are all around ω_p, which supposes a slight mode pulling, then $\omega_d^2-\omega_d'^2\sim(\omega_d-\omega_d')2\omega_d'$ and one can easily approach the frequency pulling by

$$\omega_d-\omega_d'=\frac{1}{2t_d}\frac{\mathcal{C}}{\mathcal{S}}\ . \quad (43)$$

This will be the case when ϕ is around $\pi/2$ (mod π). If the ratio $\mathcal{C}/\mathcal{S}$ diverges, then the expression $\omega_d^2-\omega_d'^2\sim\omega_d^2-\omega_p^2$ takes very large values and this supposes a very strong mode pulling effect.

We shall evaluate expression (43) to derive the frequency shift using the exact formulas given by Eqs. (34) and (37). A general idea of the behavior of such a ratio versus its parameters can be derived by taking ponctual situations. For example, when $\phi=\pm\pi/2$, $\psi_d(z)=\psi_d(0)$, and $\mathcal{C}=0$, then $\omega_d=\omega_d'$ and no frequency pulling occurs. An

analytic form of the ratio $\mathcal{C}/\mathcal{S}$ can be obtained when $f_d=1$ (two-plane-wave mixing) and for small f_d. These results are presented in Appendix B.

We have analyzed the ratio $\mathcal{C}/\mathcal{S}$ [and $\mathcal{C}^{(0)}/\mathcal{S}^{(0)}$ of Eq. (B3)] versus the main parameters: ϕ the phase mismatch between the material and the field gratings and m the ratio of the oscillating intensity on the pump intensity at the crystal input (or crystal length, respectively). The numerical investigation of Eqs. (42) and the first order of the expanded form (B1) leads qualitatively to the same conclusions: the presence of some divergence in the exact calculation appears also at the lowest order of any related expansion. The most global view on the evolution of this ratio can be obtained, however, by analyzing the approximated case. The results that we shall present need some definitions.

We call a pole a double increase of the ratio to "infinity": the appearance of a sharp line to plus (or minus) infinity followed by a second sharp line to minus (or plus) infinity defines then a narrow domain of ϕ for which the frequency shift presents very important variations. When a parameter is varied, the pole appears very progressively. It can also change its "sign": the positive (negative) infinite branch becomes the negative (positive) infinite one. As shown previously, for $\phi=\pm\pi/2$ the ratio is always zero and the frequency shift cancels. At least two poles, P_1 and P_2, for $\phi\approx 0$ ($=0$ in the approximated case) and $\phi\approx\pi$ always exist when we represent the ratio $\mathcal{C}/\mathcal{S}$ (or the frequency shift) versus the parameter ϕ. The creation of new poles occurs in the surroundings of $\phi=0$ and π by pairs (for example, a pole minus-plus and plus-minus): we call that a double pole. As the parameter is increased the poles move along the ϕ axis.

We shall present the successive form of the ratio $\mathcal{C}^{(0)}/\mathcal{S}^{(0)}$ vs ϕ when L is increased from very small values (10^{-3} cm) to $L=1$ cm. We have chosen this approximated case because one can get the full description for reasonable values of the parameters. The following observations of the behavior of the ratio $\mathcal{C}/\mathcal{S}$ are displayed on Figs. 5 and 6. The limits of the ϕ space are $-\pi/2$ and $+3\pi/2$, keeping in mind the periodicity of the diagrams. For $L<0.19$ cm, only P_1 and P_2 are present in $\phi=0$ and π. As L increases, the poles move away from each other. Then, symmetrically with respect to $\phi=\pi/2$, two opposite (one positive and one negative) growths of the ratio appear. For $L\approx 0.24$ cm, in each curve deformation double pole appears whose components then move away from each other: as L increases, the motion in the double pole seems to be strictly repulsive. When the poles are uniformly distributed with respect to ϕ for $L\approx 0.32$ cm, the closest poles to P_1 and P_2 change their signs (see above) ($L\approx 0.35$ cm), leading to the constitution of a double pole with the P's and their immediate neighbor. The general motion of the poles (except P_1 and P_2) occurs then in the opposite direction: in the double poles, the components have to move away and the four central poles start to gather around $\phi=\pi/2$. For $L\approx 0.53$ cm, the ϕ distance between the components of the double pole is large enough, and near $\phi=0$ and π a new decrease and increase appear, respectively. New double poles are present for $L\approx 0.6$ cm and the previous

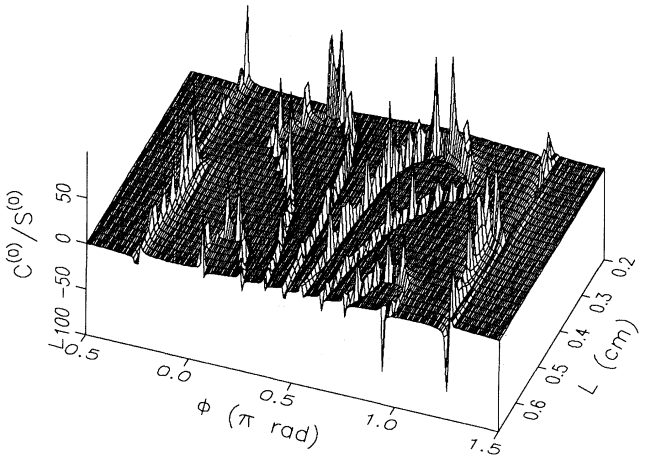

FIG. 5. Evaluation of the ratio $\mathcal{C}^{(0)}/\mathcal{S}^{(0)}$, zero order of the f_d expansion given by Eq. (B3), for various crystal lengths. We note the creation and growth of the double poles.

scenario repeats itself. For large L one can see a concentration of poles around $\phi=\pi/2$ and a creation of a pair of double poles between P_1 and P_2 and these poles bunch. In Fig. 5 one can observe the creation of two double poles, their evolution as L is varied, the change of sign, and the creation of a second pair of poles. In Fig. 6 the same previous elements are reported following only the trace of the poles (a view from above).

When $f_d\neq 0$, the analysis parameters are ϕ, and m is the intensity ratio. We have fixed the cavity length to 1 cm and observed qualitatively the above scenario, but for decreasing m values: the pole bunching is present for very low values of m, and the parameters L and m play opposite roles. This result can be deduced from the rela-

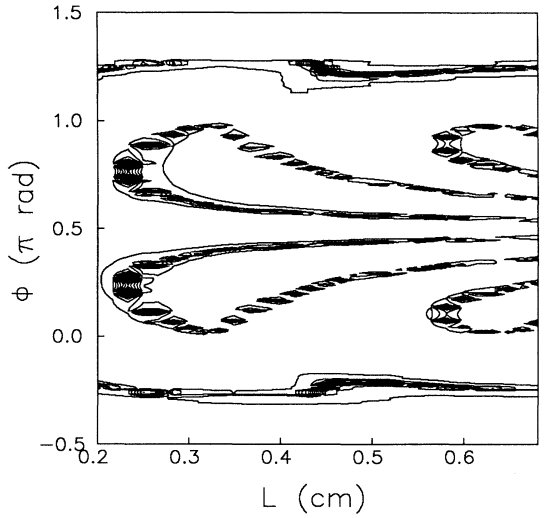

FIG. 6. Same as Fig. 5, but the exact ratio $\mathcal{C}/\mathcal{S}$ is calculated for $f_d=0.0776$. The crystal length L is taken equal to unity and replaced by the parameter m, the ratio of the oscillating beam on the pump beam at the crystal entrance.

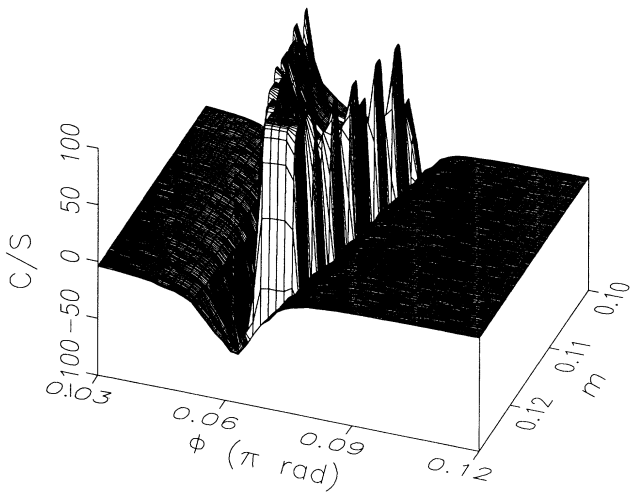

FIG. 7. The ratio $\mathcal{C}/\mathcal{S}$ vs ϕ and m for $f_d=0.0776$.

tion (B2) where these two parameters always appear via the relation $e^{-\eta L'}+m$. Moreover, the poles P_1 and P_2 seem fixed (their motion is, in fact, imperceptible when m decreases). The nascent poles are already present for $m=1$, but appear clearly for $m=0.1$. Figure 7 displays all these features.

VI. CONCLUSIONS

We give in this paper a suitable justification of the experimental observations in [16,17]: as soon as the frequency shift occurs, the transverse mode moves towards the crystal gain line frequency region, centered around the pump frequency (ω_p), and then is allowed to oscillate. From the physical point of view, the frequency pole has no meaning; it just represents large absolute increases of the mode frequency and shows that arbitrarily large shifts may be realized bringing in resonance passive modes of the cavity which were detuned from the gain profile by large amounts. This is necessary to allow several transverse modes to oscillate simultaneously in a nondegenerate cavity. Our description is a monomode one. A (active) degenerate bimode description is now in progress to follow the evolution of the poles, and such large frequency shifts should remain in that case.

This model is a first step towards a dynamical description of the photorefractive oscillator avoiding the mean-field limit (or the weak-field approximation): in that case one has to separate what happens inside the crystal from the field-cavity behavior. This explains the exhaustive study of the beam passage through the crystal: the result is that because of the transverse intensity distribution, the exchanges inside the crystal are reinforced. We expect that the intense interaction inside the crystal is a non-negligible phenomena and it can explain the experimental observations such as periodic alternance and chaotic itinerancy. Our study is also realized in the long-time limit, and the ratio m is fixed. In a dynamical description this parameter may become time dependent: during the round-trips one has to integrate the effective gain inside the crystal and the losses in the cavity; then the ratio m can be different from one lap to the following (then time dependent) until the steady state is reached. If one supposes that this state is never reached or dynamically any steady state is stable, then the system continuously evolves between its possible steady states (the cavity modes). Our present investigations are oriented in that direction.

ACKNOWLEDGMENTS

The authors wish to thank Professor P. Glorieux and Professor D. Dangoisse for fruitful discussions and their encouragement. The Laboratorie de Spectroscopie Hertzienne is "associé au CNRS."

APPENDIX A

We can get more analytical information from Eqs. (34) and (37) by treating two limiting cases.

1. Mixing two plane waves

This case is characterized by $f_d=1$ and the solutions are well known [11]. We remind the reader of the expressions of both intensities and phases:

$$I_0(z')=I_0(0)\frac{1+m}{1+me^{\eta z'}}e^{-\alpha z'}\ ,$$
$$I_d(z')=I_d(0)\frac{1+m}{e^{-\eta z'}+m}e^{-\alpha z'}\ , \tag{A1}$$

$$\psi_0(z')-\psi_0(0)=\{\psi_d(z')-\psi_d(0)\}-\eta' z'\ ,$$
$$\psi_d(z')-\psi_d(0)=\frac{\eta'}{\eta}\ln\left\{\frac{1+m}{e^{-\eta z'}+m}\right\}\ . \tag{A2}$$

These intensities and phases are also given in Figs. 3 and 4 (lower curves).

2. Mixing a plane wave and a transverse cavity mode

We can use the presence of a small parameter (f_d) following Table I, the order zero of the f_d expansion representing the second limiting case. We consider the expansions

$$\bar{I}_d(z')=\bar{I}_d^{(0)}(z')+f_d\bar{I}_d^{(1)}(z')+o(f_d^2)\ ,$$
$$K'=K_0+f_dK_1\ , \tag{A3}$$

where

$$K_0=\bar{I}_d(z'=0)=\bar{I}_d(0)=I_d(0)\ ,$$
$$K_1=-\bar{I}_d(0)\ln\left[\frac{K-\bar{I}_d(0)}{K}\right]=I_d(0)\ln[m+1]\ . \tag{A4}$$

Replacing Eqs. (A3) and (A4) in Eq. (34), one easily gets

$$\bar{I}_d^{(0)}(z')=K_0e^{\eta z'}\ ,$$
$$\bar{I}_d^{(1)}(z')=K_1e^{\eta z'}+K_0e^{\eta z'}\ln\left[1-\frac{K_0}{K}e^{\eta z'}\right]\ . \tag{A5}$$

In terms of the intensity variables, the expanded solutions of Eq. (27) are

$$I_d(z')=I_d(0)e^{(\eta-\alpha)z'} \times[1+f_d\{\ln(m+1-me^{\eta z'})\}+o(f_d^2)] , \quad \text{(A6)}$$

$$I_0(z')=[I_0(0)+I_d(0)]e^{-\alpha z'}-I_d(z') .$$

At this level we must note that the convergence of such an expansion places a strong condition on the crystal length: $\ln(m+1-me^{\eta z'})$ must take order one values with respect to the small parameter f_d. As z' increases along the crystal, this negative function increases rapidly in absolute values. To limit this growth and avoid the divergence, one needs $\xi < m+1-me^{\eta z'} < 1$ with ξ of order 10^{-4}. We easily obtain that z' has to be strictly below $z'_{\max}$, defined by $\eta z'_{\max}=\ln[(m+1)/m]$. This last relation provides the condition of a total intensity transfer between the beams for low losses: $I_d(L)=I_d(0)+I_0(0)$. Using the smallness of ξ, the analytic expression leading to z' is

$$\eta z' = \ln\left[\frac{m+1}{m}\right]-\frac{\xi}{m+1}-o(\xi^2) .$$

From the technical point of view, depending on the gain parameter η and the initial intensities ratio m, one can deduce the maximum crystal length to never exceed (for example, when η is around 10 cm^{-1}) $z'_{\max}=0.12$ cm for $m=50\%$ while $z'_{\max}=0.3$ cm for $m=5\%$.

APPENDIX B

We present the integral calculation ($\mathcal{C}$ and $\mathcal{S}$) in the two limiting cases for which the exact (or expanded analytic) expressions of the fields exist.

1. Case of two plane waves mixing

For $f_d=1$, the exact expressions of the $\mathcal{C}$ and $\mathcal{S}$ coefficients are

$$\mathcal{C}_1=\frac{\sqrt{(1+m)I_d(0)}}{\cos(\theta)} \times\int_0^{L'}dz'\frac{e^{(\eta-\alpha)z'/2}}{(1+me^{\eta z'})^{3/2}} \times\cos\left[\frac{\eta'}{\eta}\ln\left\{\frac{(1+m)e^{\eta z'}}{1+me^{\eta z'}}\right\}+\phi\right] ,$$

$$\mathcal{S}_1=\frac{\sqrt{(1+m)I_d(0)}}{\cos(\theta)} \times\int_0^{L'}dz'\frac{e^{(\eta-\alpha)z'/2}}{(1+me^{\eta z'})^{3/2}} \times\sin\left[\frac{\eta'}{\eta}\ln\left\{\frac{(1+m)e^{\eta z'}}{1+me^{\eta z'}}\right\}+\phi\right] , \quad \text{(B1)}$$

where L' is $L\cos(\theta)$. The ratio $\mathcal{C}_1/\mathcal{S}_1$ can be integrated for small losses. Let us take $\alpha=0$; we obtain

$$\frac{\mathcal{C}_1}{\mathcal{S}_1}=\frac{\left[\frac{(1+m)e^{\eta L'}}{1+me^{\eta L'}}\right]^{1/2}\cos\left[\frac{\eta'}{\eta}\ln\left\{\frac{(1+m)e^{\eta L'}}{1+me^{\eta L'}}\right\}+\beta+\phi\right]-\cos[\beta+\phi]}{\left[\frac{(1+m)e^{\eta L'}}{1+me^{\eta L'}}\right]^{1/2}\sin\left[\frac{\eta'}{\eta}\ln\left\{\frac{(1+m)e^{\eta L'}}{1+me^{\eta L'}}\right\}+\beta+\phi\right]-\sin[\beta+\phi]} , \quad \text{(B2)}$$

where we have defined $e^{i\beta}=[(\eta-\alpha)-2i\eta']/[(\eta-\alpha)^2+4\eta'^2]^{1/2}$.

2. Mixing a plane wave and a transverse cavity mode

Keeping in mind the smallness of the f_d parameter and the expansion (A6), we can derive a first order of Eq. (42) in terms of $\mathcal{C}^{(0)}$ and $\mathcal{S}^{(0)}$, which are integrable, and their ratio is given by

$$\frac{\mathcal{C}^{(0)}}{\mathcal{S}^{(0)}}=\frac{e^{L'(\eta-\alpha)/2}\cos(\eta'L'+\beta+\phi)-\cos(\beta+\phi)}{e^{L'(\eta-\alpha)/2}\sin(\eta'L'+\beta+\phi)-\sin(\beta+\phi)} . \quad \text{(B3)}$$

This last case corresponds to the previous one (Appendix B 1) but for $m=0$: small f_d is similar to a large intensity difference at the crystal input with two-plane-wave mixing.

[1] F. S. Chen, J. T. LaMacchia, and D. B. Frazer, Appl. Phys. Lett. **13**, 223 (1968).

[2] P. Günter, U. Flückiger, J. P. Huignard, and F. Micheron, Ferroelectrics **13**, 297 (1976).

[3] P. Günter, Ferroelectrics **22**, 671 (1978).

[4] G. C. Valley, A. L. Smirl, M. B. Klein, K. Bohnert, and T. F. Bogess, Opt. Lett. **11**, 647 (1986).

[5] R. W. Hellwarth, J. Opt. Soc. Am. **67**, 1 (1977).

[6] A. Yariv, IEEE J. Quantum Electron. **QE-14**, 650 (1986).

[7] B. Ya. Zel'dovich, N. F. Pilipetsky, and V. V. Shkunov, in *Principles of Phase Conjugation*, Springer Series in Optical Science Vol. 42 (Springer, Berlin, 1985).

[8] H. J. Eichler, P. Günter, and D. W. Pohl, in *Laser Induced Dynamic Gratings*, Springer Series in Optical Science Vol. 50 (Springer, Berlin, 1986).

[9] Q. Byron HE, Pochi Yeh, and G. GU, Opt. Lett. **17**, 664

(1992).
[10] Sze-Keung Kwong, M. Cronin-Golomb, and A. Yariv, IEEE J. Quantum Electron. **QE-22**, 1508 (1986).
[11] Pochi Yeh, IEEE J. Quantum Electron. **QE-25**, 484 (1989).
[12] For a review on the photorefractive index, see A. M. Glass, Opt. Eng. **17**, 470 (1978); J. Feinberg, in *Optical Phase Conjugation,* edited by R. A. Fisher (Academic, New York, 1983), Chap. 11.
[13] *Photorefractive Materials and Their Applications I and II,* edited by P. Günter and J. P. Huignard, Topics in Applied Physics Vols. 61 and 62 (Springer-Verlag, Berlin, 1987); J. Feinberg, D. Heiman, A. R. Tanguay, Jr., and R. W. Hellwarth, J. Appl. Phys. **53**, 1297 (1980).
[14] T. J. Hall, R. Jaura, L. M. Connors, and P. D. Foote, Prog. Quantum Electron. **10**, 77 (1985).
[15] J. Feinberg and G. D. Bacher, Opt. Lett. **9**, 420 (1984).
[16] H. Rajbenbach and J. P. Huignard, Opt. Lett. **10**, 137 (1985).
[17] F. T. Arecchi, G. Giacomelli, P. L. Ramazza, and S. Residori, Phys. Rev. Lett. **65**, 2531 (1990).
[18] J. O. White, M. Cronin-Golomb, B. Fisher, and A. Yariv, Appl. Phys. Lett. **40**, 450 (1982).
[19] D. Z. Anderson and R. Saxena, J. Opt. Soc. Am. B **4**, 164 (1987).
[20] G. D'Alessandro, Phys. Rev. A **46**, 2791 (1992).
[21] A. Yariv and Sze-Keung Kwong, Opt. Lett. **10**, 454 (1985).
[22] N. V. Kukhtarev, V. B. Markov, S. G. Odulov, M. S. Soskin, and V. L. Vinetskii, Ferroelectrics **22**, 949 (1979).
[23] H. Kogelnik and T. Li, Proc. IEEE **54**, 1312 (1966); L. A. Lugiato, G. L. Oppo, J. R. Tredicce, L. M. Narducci, and M. A. Pernigo, J. Opt. Soc. Am. B **7**, 1019 (1990).